

# Uncertainty-Aware Planning for Heterogeneous Robot Teams using Dynamic Topological Graphs and Mixed-Integer Programming

Cora A. Dimmig<sup>1,2</sup>, Kevin C. Wolfe<sup>1</sup>, Bradley Woosley<sup>3</sup>, Marin Kobilarov<sup>2</sup>, and Joseph Moore<sup>1,2</sup>

**Abstract**—Multi-robot planning and coordination in uncertain environments is a fundamental computational challenge, since the belief space increases exponentially with the number of robots. In this paper, we address the problem of planning in uncertain environments with a heterogeneous robot team of fast scout vehicles for information gathering and more risk-averse carrier robots from which the scouts vehicles are deployed. To overcome the computational challenges, we represent the environment and operational scenario using a topological graph, where the parameters of the edge weight distributions vary with the state of the robot team on the graph, and we formulate a computationally efficient mixed-integer program which removes the dependence on the number of robots from its decision space. Our formulation results in the capability to generate optimal multi-robot, long-horizon plans in seconds that could otherwise be computationally intractable. Ultimately our approach enables real-time re-planning, since the computation time is significantly faster than the time to execute one step. We evaluate our approach in a scenario where the robot team must traverse an environment while minimizing detection by observers in positions that are uncertain to the robot team. We demonstrate that our approach is computationally tractable, can improve performance in the presence of imperfect information, and can be adjusted for different risk profiles.

## I. INTRODUCTION

As multi-robot systems are deployed in real-world scenarios, capabilities for reasoning about environmental uncertainty become essential. For instance, to be successful in uncertain hazardous environments, a robot team must balance achieving mission objectives (e.g., navigating to a goal) with avoiding unforeseen hazards that could catastrophically impact team performance. However, achieving unified multi-robot planning and coordination in uncertain environments poses a significant computational challenge, since the belief space (i.e., the space of all possible probability distributions over the state space) grows exponentially with the number of robots due to accounting for robot interactions.

In this paper, we present a computationally tractable approach for planning and coordination of heterogeneous robot teams operating in uncertain environments when the robot team members possess different risk profiles. In particular, we consider the case where the multi-robot team consists of fast, risk-tolerant scout vehicles and risk-averse carrier vehicles. To create a computationally tractable decision space, we construct a dynamic topological graph structure, as seen

<sup>1</sup>Johns Hopkins University Applied Physics Laboratory, Laurel, MD 20723, USA. Email: Cora.Dimmig@jhuapl.edu, Joseph.Moore@jhuapl.edu

<sup>2</sup>Department of Mechanical Engineering, Johns Hopkins University, Baltimore, MD 21218, USA.

<sup>3</sup>DEVCOM Army Research Laboratory, Adelphi, MD 20783, USA.

Distribution statement A. Approved for public release; distribution is unlimited.

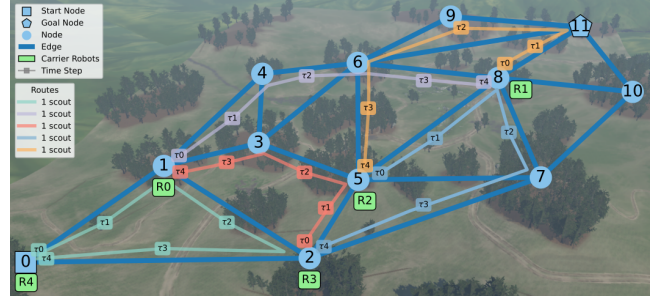


Fig. 1. A dynamic topological graph, in a meadow environment from [1] with uncertain edge weights, applied to a reconnaissance test scenario. The routes through the graph show the paths of scout agents deployed from carrier vehicles to explore the environment.

in Fig. 1, by discretizing the environment based on the operational scenario and *a priori* terrain data. The graph also embeds the critical relationship between environmental uncertainty and the state of the robot team in its stochastic edge weights. We then use this graph to formulate an optimization problem with Mixed-Integer Programming (MIP) for generating multi-robot plans that reason about uncertainty while satisfying spatial and temporal coordination constraints.

To evaluate our approach, we consider a scenario in which a heterogeneous robot team must minimize detection by observers while navigating through an environment where observer positions are dynamic and not fully known. Our numerical results demonstrate that our approach is computationally tractable for medium-sized robot teams ( $\sim 10$  agents) operating in large-scale environments and can enable adaptive re-planning as new information is received. We also detail the advantages of our approach through an ablation study that shows the value of reasoning about uncertainty, leveraging information-gathering scout robots, and including certainty decay. Unlike our prior approach in [2], the method presented in this paper can reason about environmental uncertainty, utilize heterogeneous risk profiles, and leverage rapid re-planning to adapt to new information. Our contributions are as follows:

- A novel dynamic topological graph formulation for embedding environmental uncertainty.
- A compact mixed-integer optimization problem capable of encoding graph edge uncertainty and heterogeneous teaming constraints.
- A computationally efficient approach for graph-planning that can enable online adaptation to new information and accommodate different risk profiles of the team.

## II. RELATED WORK

Multi-robot planning and coordination in uncertain environments is often posed as a multi-agent Partially Observable

Markov Decision Process (POMDP) [3]. However, even for single robot planning problems, generating an optimal solution for a POMDP is computationally intractable [4]. These computational challenges are further exacerbated for multi-robot systems, since the belief space increases exponentially with the number of robots [5]. To overcome computational limitations, researchers have employed a number of approximations and abstractions to generate sub-optimal solutions. In some cases, researchers have maintained continuous state and action representations and have relied on generating local policies in belief-space to enable multi-robot planning in unknown environments [6]. In most cases, however, researchers have relied on a discretization of the state and action space to facilitate computational tractability. For instance, many approaches decompose an overall robot team objective (e.g., exploration) into discrete sub-tasks. Task assignment and planning are often decoupled, where individual robots execute local policies while auction-based methods allocate tasks [7], [8]. In [5], the authors use auctions to allocate POMDP policies for individual robots. Other researchers discretize the action space via macro-actions [9].

Graphs have served as an effective means of discretizing state and action spaces to enable planning for single and multi-robot scenarios, including multi-agent path finding [10] and more complex coordination tasks [2], [11]. Oftentimes, nodes represent robot states while edges represent possible transitions between those states. Characteristics such as spatial or temporal relationships between tasks or robots can be embedded into the graph through properties like node connectivity and edge weights. Graphs have also proven to be useful for planning in uncertain environments, with researchers modeling uncertain edge weights as binary [12] or continuous random variables [13], [14], whose distribution could be dependent on decisions made at a prior node [15].

To generate plans on these graphs, researchers have explored search-based, learning-based, and optimization-based approaches. Most search-based approaches have been developed for single robots (e.g., [16]), while some conflict-based search approaches have been developed for multi-robot systems to address task completion uncertainty or stochastic travel times [17], [18]. To overcome challenges associated with problem scale, machine learning methods have been applied. In [19], [20], researchers learn policy graphs to coordinate macro actions to solve a decentralized POMDP. In [21], a graph structure is used with approximate policy iteration for a multi-robot repair problem. Recently, Graph Neural Networks (GNNs) have been investigated toward multi-robot coordination in uncertain environments [22], [23]. Advances in optimization, specifically MIP, have also enabled single robot [24] and multi-robot [25], [26] planning in unknown environments using a graph structure, but all report computational challenges.

Although most of the research on the planning and coordination of multi-robot teams under uncertainty has explored homogeneous teams, researchers have also explored planning for heterogeneous teams using both MIP techniques [27]–[30] and learning-based approaches [31], [32]. One advantage of heterogeneous robot teams is their ability to more

effectively distribute risk across the team [33].

In this paper, we present an approach that uses a graph structure and MIP to enable risk-aware planning for heterogeneous multi-robot teams under environmental uncertainty. Contrary to the multi-robot routing problem, we assume that multiple agents can simultaneously traverse an edge. Similar to [16], we model our edge costs as random variables whose values can be uncovered via exploration. We employ a heterogeneous robot team, where each robot class possesses a different risk profile that dictates the class’s tolerance for being detected. Our carrier robots are more risk-adverse, since they are responsible for the underlying goal of the scenario (with the aid of scout robots) and thus their detection would be more significant. To solve for a multi-robot plan, we use a compact MIP formulation. In our prior research [2], we used a similar approach to generate multi-robot plans for a homogeneous multi-robot team on a topological graph with deterministic edge costs. Here, we present an approach to address the challenges posed by coordinating a heterogeneous team in uncertain environments.

### III. PROBLEM STATEMENT

We consider the problem of planning and coordination for a heterogeneous robot team by generating a graph  $G = (V, E, w_e)$ , with nodes  $v \in V$  and edges  $e \in E$ , based on the critical features of the planning problem. The edge cost  $w_e : E \times X \times T \rightarrow \mathbb{R}_{>0}$  is a bounded random variable that depends on the underlying environmental uncertainty  $u_e \in [u_e^-, u_e^+]$ , the discrete robot team state on the graph  $x \in X$ , and time  $t \in \mathbb{R}_{>0}$ . We consider  $n_{CL}$  robot classes and  $n_E$  total edges such that  $X = X^1 \times X^2 \times \dots \times X^{n_{CL}}$ , where  $X^i = \{[p_{e_1}^i, p_{e_2}^i, \dots, p_{e_{n_E}}^i] \in \mathbb{Z}_{>0}^{n_E}\}$  and  $p_{e_j}^i$  is the number of robots of class  $i$  on edge  $e_j$ . We assume a level of abstraction where multiple robots may simultaneously traverse an edge. We also allow robots to uncover the true edge cost by inspecting an edge. Following an inspection, we assume that the edge cost uncertainty returns to its original value after a finite time.

We furthermore let each robot class  $i$  be constrained to graph  $G^i = (V^i, E^i, w_e^i)$ , where  $V^i \subseteq V$ ,  $E^i \subseteq E$ , and  $w_e^i(e^i, x, t^i) = \zeta^i w_e(e^i, x, t^i)$  for  $e^i \in E^i$ ,  $x \in X$ , and  $t^i \in [1, n_\tau^i]$ . We can now capture heterogeneous mobility, cost, speed, and sensing characteristics by defining for each robot class a graph  $G^i$ , an edge cost scale factor  $\zeta^i$ , and traversal time factor  $n_\tau^i$ . We also permit a set of costs and constraints that govern inter-class interactions.

#### A. Reconnaissance Test Scenario

In this paper, we consider a particular reconnaissance test scenario where a heterogeneous team of robots must traverse an environment while minimizing detection by observers whose exact positions are unknown. We assume that our graph  $G$  can be generated using a visibility metric computed from a distribution over observer locations, similar to [34], where nodes are assigned to low visibility regions and edge costs embed probability of detection. Thus, the distribution over observer locations gives rise to uncertain edge weights.

In this scenario, we assume that the observer position can change incrementally over time, such that the true edge costs uncovered from inspecting an edge have the highest certainty in the first time step following an inspection and become less certain as time progresses. Instead of modeling observer dynamics explicitly, we attempt to capture observer behavior implicitly through the temporal growth of edge cost uncertainty after an inspection.

We restrict our robot team to two classes: carrier robots and scout robots. Scout robots move more quickly than carrier robots, incur less cost, and possess sensors for inspecting edges to reduce uncertainty bounds to zero. Carrier robots can carry at most one scout robot. Scouts can deploy when the carrier robots are at nodes and return within one carrier robot time increment to any empty carrier robot. When a scout vehicle is deployed from a carrier robot, it incurs a specified deployment cost. In this paper, the edge cost scale factor for carrier robots and scouts are 1 and  $\zeta$ , respectively, and the traversal time factors are 1 and  $n_\tau$ , respectively. We also assume that all robots operate on graphs with identical sets of vertices and edges, i.e.,  $E^i = E$ ,  $V^i = V$ ,  $\forall i$ .

Given the constraints of this robot team, our overall objective is to minimize the total cost incurred by the team when the edge costs are uncertain. To do so, we define a cost that adequately captures the underlying uncertainty. We model our uncertain edge costs using bounded uncertainty; thus, we can use the Hurwicz Criterion [13], [35] as part of our objective function. The Hurwicz Criterion was developed for decision making under interval uncertainty to balance pessimism and optimism by considering both the best and worst possible outcomes [36]. We define a ‘‘coefficient of optimism,’’  $\beta \in [0, 1]$ , that is set based on the tolerance of the outcome. Then for a condition  $c$  we want to minimize, which is bounded such that  $c^{\downarrow} \leq c \leq c^{\uparrow}$ , the Hurwicz Criterion leads to the minimization of a cost of the following form.

$$\beta c^{\downarrow} + (1 - \beta) c^{\uparrow} \quad (1)$$

For  $\beta = 1$ , this criterion expresses complete optimism and for  $\beta = 0$ , this criterion expresses complete pessimism.

#### IV. MIXED INTEGER PROGRAMMING APPROACH

Rather than pursuing a search-based or learning-based solution to the multi-robot planning and coordination problem, we adopt an optimization-based approach where the costs and constraints can be directly encoded. Since our problem is characterized by both discrete and continuous decision variables, we formulate the uncertainty-aware multi-robot planning problem using MIP. We introduce the parameters used in our formulation in Table I. A scenario is defined by the categories ‘‘Problem Size,’’ ‘‘Scenario Variables,’’ and ‘‘Problem Parameters’’ based on the environment of interest. These categories encompass the parameters relating to the graph connectivity, start and goal locations of the robots, and planning horizons. The ‘‘Cost of Traversing’’ and ‘‘Uncertainty’’ categories define parameters that will affect the team’s behaviors on the graph and are based on the observer’s expected location. In this work, we select values of these parameters to demonstrate the behaviors of our algorithm.

TABLE I  
MIP PARAMETERS

Category	Var	Description
Problem Size	$n_A$	Number of carrier agents/robots
	$n_K$	Number of scouts
	$n_T$	Number of time steps in the time horizon
	$n_\tau$	Number of scout time steps
	$n_E$	Number of edges, both directions
	$n_V$	Number of nodes/vertices
	$n_L$	Number of locations ( $n_E + n_V$ )
	$n_S$	Number of start locations
Scenario Variables	$E$	Set of edges $e$
	$V$	Set of nodes/vertices $v$
	$L$	Set of locations $l$ consisting of edges and vertices, $E \cup V$
	$S$	Set of start locations $s$ , $S \subseteq L$
Problem Parameters	$t$	Time step from 1 to $n_T$
	$\tau$	Scout time step from 1 to $n_\tau$
	$n_s$	Number of robots at start location $s \in S$
	$n_d$	Number of robots at goal location $d \in D$
Cost of Traversing	$\bar{w}_e$	Expected cost to traverse edge $e \in E$
	$r_e$	Cost reduction on $e$ for teaming
	$\zeta$	Scout edge cost reduction
	$\eta_v$	Cost of scout launch from node $v \in V$
Uncertainty	$u_e^{\downarrow}$	Lower bound on uncertainty of edge $e \in E$
	$u_e^{\uparrow}$	Upper bound on uncertainty of edge $e \in E$
	$\xi$	Scale of uncertainty for all edges versus traversed edges
	$\lambda$	Time horizon for inspections to decay
	$\beta$	Coefficient of optimism

TABLE II  
MIP DECISION VARIABLES (AT TIME  $t$ )

Variable	Type	LB	UB	Description
$p_{l,t}$	Int	0	$n_A$	Number of robots at location $l$
$\phi_{e,t}$	Bin	0	1	Whether robots are on edge $e$
$\psi_t$	Bin	0	1	Whether robots have moved
$q_{l,\tau,t}$	Int	0	$n_K$	Number of scouts at $l$ at time $\tau$
$\theta_{e',t}$	Bin	0	1	Whether scouts are on $e'$ at time $\tau$
$f_{v,t}$	Int	0	$n_K$	Number of scouts deployed from $v$
$\delta_{e',t}$	Bin	0	1	Whether edge $e'$ was inspected
$z_{e',t}$	Cont	0	1	Inspection ratio for edge $e'$
$C_{U_{A_e},t}$	Cont	0	$\infty$	Carrier cost of uncertainty for $e$
$C_{U_{K_{e'},t}}$	Cont	0	$\infty$	Scout cost of uncertainty for $e'$

Our total number of robots is  $n_A + n_K$ , carriers and scouts. To represent the accelerated speed of the scouts, the scouts operate with time step  $\tau$ . During one time step  $t$  for the carrier robots there are  $n_\tau$  scout time steps  $\tau$ .

Table II presents the categories of decision variables we employ as well as their type (integer, binary, or continuous), bounds (lower (LB) and upper (UB)), and descriptions. The key decision variables  $p_{l,t}$  for carrier robots and  $q_{l,\tau,t}$  for scout robots track the number of robots at a particular location  $l$  at each time step  $t$  (and for scouts, scout time step  $\tau$ ). After a solution is generated to the MIP problem, an assignment routine can be performed to construct the path

each robot takes from these variables.

For an undirected graph, we consider both directions of each edge in  $E$  to be equivalent. In some cases, we can consider the set of only one direction of each edge,  $E'$ , with element  $e' \in E'$ . To remove extraneous variables, scout decision variables exclude the last time step  $t = n_T$  and potentially the first time step if their deployment is delayed. We use  $t'$  to distinguish cases with a truncated time horizon. In Table II, we denote these cases with  $e'$  and  $t'$ . For brevity, we drop this notation in our derivation.

### A. Mathematical Preliminaries

In this work, we add slack variables and constraints to express nonlinear terms of our cost functions linearly, ultimately yielding a Mixed-Integer Linear Program (MILP). We strive to minimize the number of additional variables and constraints added since these impact the overall solve time of the MILP. To do this, we exploit the conclusions in [37], [38] to transform a quadratic cost term into a linear cost term with linear constraints using a slack variable.

**Proposition 1:** If  $\alpha \in \{0, 1\}$  is a binary variable,  $b \in \mathbb{R}$ , and  $h(b)$  is a linear function with bounds  $h^{\lfloor} \leq h(b) \leq h^{\lceil}$ , then minimizing  $\alpha h(b)$  is equivalent to  $\min y$  for slack variable  $y \in \mathbb{R}$  with the following constraints.

$$\alpha h^{\lfloor} \leq y \leq \alpha h^{\lceil} \quad (2)$$

$$h(b) - h^{\lceil}(1 - \alpha) \leq y \leq h(b) - h^{\lfloor}(1 - \alpha) \quad (3)$$

**Corollary 1:** When minimizing, if all other constraints are independent of  $y$  and the coefficient of  $y$  in the cost function is nonnegative, then only the left side constraints are structural, and thus necessary for optimization.

$$y = \max\{\alpha h^{\lfloor}, h(b) - h^{\lceil}(1 - \alpha)\} \quad (4)$$

$$\leq \min\{\alpha h^{\lceil}, h(b) - h^{\lfloor}(1 - \alpha)\} \quad (5)$$

**Special Case 1:** For a constant  $a \geq 0$ ,  $h(b) = 1 - b$ ,  $b \in [0, 1]$ , and thus  $h^{\lfloor} = 0$  and  $h^{\lceil} = 1$ , the minimization of  $a\alpha(1 - b)$  can be equivalently expressed as follows.

$$\min y \text{ s.t. } y \geq a(\alpha - b), y \geq 0 \quad (6)$$

**Proposition 2:** For  $b \in [0, b^{\lceil}]$ , an indicator variable  $\alpha \in \{0, 1\}$  can be expressed as follows, for any constant  $a \geq 0$ .

$$\alpha = \begin{cases} 1, & b > 0 \\ 0, & b = 0 \end{cases} \Leftrightarrow \min a\alpha \text{ s.t. } \alpha \geq \frac{b}{b^{\lceil}} \quad (7)$$

### B. Heterogeneous Team and Uncertainty Cost Functions

The main objective in our reconnaissance test scenario is to minimize detection by observers and the time to reach a goal location(s). We represent a vehicle's detectability through edge costs incurred while traversing the graph, with associated uncertainty values to represent the stochasticity in our prediction of the observer's location. We compose a cost function with four categories, which we derive in the following sections: traversing ( $C_{W_{e,t}}$ ), uncertainty ( $C_{U_{e,t}}$ ), launching scouts ( $C_{F_{v,t}}$ ), and time ( $C_{T_t}$ ). We sum these terms across all time steps to represent the overall objective function value  $C$ , which we aim to minimize. Each of these

terms can be scaled based on the priorities of a scenario (e.g., minimizing detection versus the time to reach the goal).

$$C = \sum_{t=1}^{n_T} \left( C_{T_t} + \sum_{e \in E} (C_{W_{e,t}} + C_{U_{e,t}}) + \sum_{v \in V} C_{F_{v,t}} \right) \quad (8)$$

1) *Cost of Traversing and Uncertainty:* We first consider, for each time step  $t$ , the uncertain cost of traversing edge  $e$ ,  $\tilde{C}_{W_{e,t}}$ , that is equal to the weight on the edge,  $w_e$ , if any carrier vehicles are on that edge plus a scaled weight  $\zeta w_e$  for each scout on that edge. We consider  $w_e$  to be a random variable with an expected value of  $\bar{w}_e$  and interval uncertainty. We add the scaling factor  $\zeta$  to represent a difference in cost for scouts versus carrier vehicles to traverse the edge (e.g., scouts movement may be less risky due to their increased speed). We apply the cost  $w_e$  once for carrier robots since they traverse as a team and, when traversing separately,  $\zeta w_e$  for each scout vehicle because they move independently. We track whether carrier vehicles are traversing edge  $e$  with the binary variable  $\phi_{e,t}$  and, for each scout time step  $\tau$ , how many scouts are traversing edge  $e$  with integer variable  $q_{e,\tau,t}$ .

$$\tilde{C}_{W_{e,t}} = w_e \left( \phi_{e,t} + \zeta \sum_{\tau=1}^{n_\tau} q_{e,\tau,t} \right) \quad (9)$$

Let the upper bound of  $w_e$  be  $\bar{w}_e + u_e^{\lceil}$  and the lower bound be  $\bar{w}_e - u_e^{\lfloor}$ . We can then apply (1) to define  $\hat{w}_e = \beta(\bar{w}_e - u_e^{\lfloor}) + (1 - \beta)(\bar{w}_e + u_e^{\lceil})$ .

After reorganizing terms, this results in  $\bar{w}_e$  plus an expression dependent on the uncertainty bounds,  $\hat{u}_e = (1 - \beta)u_e^{\lceil} - \beta u_e^{\lfloor}$ . By letting  $w_e \approx \hat{w}_e$ , we can derive a cost based on (9) that, if minimized, satisfies the Hurwicz Criterion.

$$\hat{C}_{W_{e,t}} = \bar{w}_e \left( \phi_{e,t} + \zeta \sum_{\tau=1}^{n_\tau} q_{e,\tau,t} \right) + \hat{u}_e \left( \phi_{e,t} + \zeta \sum_{\tau=1}^{n_\tau} q_{e,\tau,t} \right) \quad (10)$$

**Cost of Traversing:** The first term in (10) is an expression of the expected cost of traversing. In our final cost of traversing  $C_{W_{e,t}}$ , we add a linear cost reduction  $r_e$  based on the number of agents on the edge  $p_{e,t}$  as a risk reduction when multiple carrier vehicles traverse together, as in [2].

$$C_{W_{e,t}} = \bar{w}_e \phi_{e,t} - r_e p_{e,t} + \zeta \bar{w}_e \sum_{\tau=1}^{n_\tau} q_{e,\tau,t} \quad (11)$$

**Cost of Uncertainty:** The second term in (10) is the impact of the uncertainty  $u_e$  on the cost of traversing edge  $e$  at time  $t$ . We add a term to this expression for the total uncertainty across all edges, scaled by  $\xi$ , to encourage general exploration by the scouts (rather than focused exploration on edges intended to be traversed), in case new information would reveal a superior path. Together, these terms form an expression for the maximum cost of uncertainty as follows.

$$\hat{u}_e \left( \xi + \phi_{e,t} + \zeta \sum_{\tau=1}^{n_\tau} q_{e,\tau,t} \right) \quad (12)$$

The role of the scouts in our formulation is to reduce uncertainty by exploring edges ahead of the rest of the team. To reflect this, we add a ratio  $z_{e,t}$  for how recently

an edge has been inspected. We use this ratio to reduce the uncertainty of explored edges (i.e., the incurred cost of uncertainty is  $\hat{u}_e(1 - z_{e,t})$ ). The ratio  $z_{e,t}$  is 0 if the edge has not yet been inspected and 1 when the edge was inspected at  $t - 1$ . The value of  $z_{e,t}$  decays over time to reflect how recently the scouts explored an edge. Additionally, when running with a receding horizon, the collected data can be used to update the values of the edge weights and uncertainty.

During a carrier robot time step  $t$ , after scouts explore an edge for the first time, the scouts no longer incur the cost of uncertainty on additional passes of that particular edge during time  $t$ . The scouts gathered full knowledge of that edge for time  $t$  in their first pass. To enforce this paradigm, we replace  $\sum_{\tau=1}^{n_\tau} q_{e,\tau,t}$  in (12) with decision variable  $\theta_{e,t}$ , which tracks whether scouts use an edge  $e$  at time  $t$ .

We combine the reduction in uncertainty due to  $z_{e,t}$  and the use of  $\theta_{e,t}$  with the expression in (12) to calculate our overall cost of uncertainty for a particular edge  $e$  at time  $t$ .

$$C_{U_{e,t}} = \hat{u}_e(\xi(1 - z_{e,t}) + (\phi_{e,t} + \zeta\theta_{e,t})(1 - z_{e,t})) \quad (13)$$

The expression in (13) is nonlinear in the decision variables. To formulate (13) as a linear cost with linear constraints, we first break this expression into a linear component and two cost terms  $C_{U_{A_{e,t}}}$  and  $C_{U_{K_{e,t}}}$ .

$$C_{U_{e,t}} = \hat{u}_e\xi(1 - z_{e,t}) + C_{U_{A_{e,t}}} + C_{U_{K_{e,t}}} \quad (14)$$

$$C_{U_{A_{e,t}}} = \hat{u}_e\phi_{e,t}(1 - z_{e,t}) \quad (15)$$

$$C_{U_{K_{e,t}}} = \zeta\hat{u}_e\theta_{e,t}(1 - z_{e,t}) \quad (16)$$

In our test case, our aim is to be risk-averse, so we can assume  $u_e^\square < u_e^\square$  and  $\beta < 0.5$  to ensure  $\hat{u}_e \geq 0$  for all edges  $e$ . We can then apply *Special Case 1* from Sec. IV-A, by using the cost terms  $C_{U_{A_{e,t}}}$  and  $C_{U_{K_{e,t}}}$  as slack variables with lower bounds of 0. We add the following constraints.

$$C_{U_{A_{e,t}}} \geq \hat{u}_e(\phi_{e,t} - z_{e,t}) \quad (17)$$

$$C_{U_{K_{e,t}}} \geq \zeta\hat{u}_e(\theta_{e,t} - z_{e,t}) \quad (18)$$

Following *Special Case 1*,  $C_{U_{A_{e,t}}}$  and  $C_{U_{K_{e,t}}}$  will be strict to the minimum possible values given the constraints, and thus can replace (15) and (16). Overall, this constraint formulation allows the cost of uncertainty to remain linear with linear constraints, which significantly improves solve time.

2) *Cost of Launch*: To represent the risk associated with deploying a scout vehicle (e.g., an aerial vehicle may be noticeable and noisy), we introduce a cost for launching the vehicle,  $C_{F_{v,t}}$ . The launch cost for a particular vertex,  $\eta_v$ , is the average cost of the surrounding edges multiplied by a scaling factor. We express the cost for all  $t$  and  $v$ .

$$C_{F_{v,t}} = \eta_v f_{v,t} \quad (19)$$

3) *Cost of Time*: To quantify the risk associated with the time to reach a goal, we formulate a linear cost of time  $C_{T_t}$  for each time step  $t$ , as in [2]. We introduce binary decision variables  $\psi_t$  that track whether any robots have moved on the graph at time  $t$  and scale this value by the current time  $t$ , such that the cost increases the longer the robots are traversing.

$$C_{T_t} = t\psi_t \quad (20)$$

### C. Scout and Uncertainty Constraints

1) *Time Tracking Variables*: We define a constraint for the time tracking variables  $\psi_t$ . A robot would not pause on an edge due to the edge's weight, thus being on an edge implies movement. In the overall cost function,  $\psi_t$  only contributes to increasing cost, so we constrain  $\psi_t$  using *Proposition 2* from Sec. IV-A, such that  $\psi_t = 1$  when any number of robots move on an edge and otherwise  $\psi_t = 0$ .

$$\psi_t \geq \frac{1}{n_A + n_K n_\tau} \sum_{e \in E} \left( p_{e,t} + \sum_{\tau=1}^{n_\tau} q_{e,\tau,t} \right) \quad (21)$$

2) *Carrier Robot and Scout Edge Used Variables*: We define binary variables  $\phi_{e,t}$  and  $\theta_{e,t}$  to track if edge  $e$  is being traversed by the carrier robots and scouts, respectively, at time  $t$ . Since  $\phi_{e,t}$  and  $\theta_{e,t}$  contribute to increasing the cost function, we define constraints using *Proposition 2*.

$$\phi_{e,t} \geq \frac{1}{n_A} p_{e,t}, \quad \theta_{e,t} \geq \frac{1}{n_K n_\tau} \sum_{\tau=1}^{n_\tau} q_{e,\tau,t} \quad (22)$$

3) *Start and Destination Constraints*: We add constraints for the start and destination locations of the overall robot team using the carrier robot locations. The number of robots at each start location  $s$  is  $n_s$  and the minimum number of robots at each destination location  $d$  is  $n_d$ .

$$p_{s,1} = n_s, \quad p_{d,n_T} \geq n_d \quad (23)$$

4) *Scout Deployment Constraints*: Scouts must launch from a carrier robot and return to a carrier robot without a scout. We use decision variables  $f_{v,t}$  to track the number of scouts deployed from a particular location  $v$  at time step  $t$ . We bound this value based on the number of carrier robots at that location. Additionally, we add start and goal constraints to deploy and return to those locations. For all  $t$  and  $v$ , we add the following constraints.

$$f_{v,t} \leq p_{v,t}, \quad q_{v,1,t} = f_{v,t}, \quad q_{v,n_\tau,t} = f_{v,t} \quad (24)$$

5) *Maximum Robots*: We constrain the maximum number of carrier robots across all locations at all time  $t$  to be equal to the total number of carrier robots. Similarly, we constrain the maximum number of scouts across all locations at all  $\tau$  and  $t$  to be equal to the number of scouts deployed.

$$\sum_{l \in L} p_{l,t} = n_A, \quad \sum_{l \in L} q_{l,\tau,t} = \sum_{v \in V} f_{v,t} \quad (25)$$

6) *Carrier Robot and Scout Sequential Flow Constraints*: To restrict the carrier robots and scouts movement to the topological graph, we add flow constraints for each vehicle type. For each node  $v_j$ , we constrain the number of robots entering the node and in the node to be equal to the number of robots in the node and leaving the node in the next time step. For the carrier robots, we add constraint (26) for all  $t \in [2, n_T]$  and node  $v_j$ . For the scouts, we add constraint (27) for all  $t, \tau \in [2, n_\tau]$ , and node  $v_j$ .

$$\sum_{l_{ij}=(v_i,v_j) \in L} p_{l_{ij},t-1} = \sum_{l_{ji}=(v_j,v_i) \in L} p_{l_{ji},t} \quad (26)$$

$$\sum_{l_{ij}=(v_i,v_j) \in L} q_{l_{ij},\tau-1,t} = \sum_{l_{ji}=(v_j,v_i) \in L} q_{l_{ji},\tau,t} \quad (27)$$

In each constraint, the first sum tracks the number of robots on edges entering node  $v_j$  (i.e., locations of the form  $l_{ij} = (v_i, v_j)$ ) and the second sum tracks the number of robots on edges exiting  $v_j$  (i.e., locations of the form  $l_{ji} = (v_j, v_i)$ ). Both sets of locations include the node (i.e., location  $l_{jj}$ ), as all nodes have self-loops. Since the cost on the edges is greater than zero, the cost function ensures the robots will not stay on an edge, and thus being on an edge implies that the robot is headed to the corresponding node.

7) *Edge Inspection Variables*: We add constraints for the binary decision variables  $\delta_{e,t}$  to track which edges the scouts have traversed to inspect. For  $e$  and  $t = [1, n_T - 2]$ ,  $\delta_{e,t}$  tracks if edge  $e$  has been inspected at time  $t$ .

$$\delta_{e,t} \leq \sum_{\tau=1}^{n_\tau} q_{e,\tau,t} \quad (28)$$

We use  $z_{e,t}$  to track inspection ratios. If edge  $e$  was inspected in the last time step then  $z_{e,t} = 1$ . Over time  $z_{e,t}$  will decay, reflecting uncertainty increasing since the last time edge  $e$  was inspected. We denote  $\lambda$  as the number of time steps for the inspection information to decay.

We consider the uncertainty to increase logarithmically with time. By using the additive property of logarithms over our inspection horizon, our formulation ensures there is value from each inspection to encourage more frequent exploration. We approximate  $\ln(k)$  with the harmonic number  $H_k = \sum_{n=1}^k \frac{1}{n}$ . Using the series identity for the harmonic number, we can isolate the impact of an inspection at each time step in the inspection horizon.

$$\frac{1}{\lambda} \sum_{k=1}^{\lambda} H_k = \frac{1}{\lambda} ((\lambda + 1)H_\lambda - \lambda) = \sum_{t_d=1}^{\lambda} \frac{\lambda - t_d + 1}{\lambda t_d} \quad (29)$$

We then switch coordinates in (29) to be relative to the time  $t$  and use the binary  $\delta_{e,t}$  to sum components corresponding to completed inspections. In the following constraint, for all  $e$  and  $t$ , the fractional component controls the impact of each time step's information on the overall sum, with increasingly smaller values for less recent inspections.

$$z_{e,t} \leq \sum_{t_h=\max(t-\lambda,1)}^{t-1} \delta_{e,t_h} \frac{\lambda - (t - t_h) + 1}{\lambda(t - t_h)} \quad (30)$$

Both  $z_{e,t} \in [0, 1]$  and  $\delta_{e,t} \in \{0, 1\}$  only contribute to the overall cost function (8) by reducing cost so the optimizer will seek to maximize these values. Thus, equality will be achieved in both (28) and (30) up to their maximum bounds.

#### D. Uncertainty-Aware Multi-Robot Optimization Problem

We combine our objective functions and constraints to form our overall MILP problem in Table III, which we solve with the Gurobi optimizer [39].

### V. COMPUTATIONAL RESULTS AND DISCUSSION

We evaluate our approach in scenarios that demonstrate the benefit of uncertainty reduction using scout robots. Scouts generally prioritize exploring high uncertainty edges and edges that are planned to be traversed to provide the greatest

TABLE III  
MIP OPTIMIZATION PROBLEM WITH UNCERTAINTY AND SCOUTS

	Optimization Problem	Eq.
	$\min \sum_{t=1}^{n_T} \left( C_{T_t} + \sum_{e \in E} (C_{W_{e,t}} + C_{U_{e,t}}) + \sum_{v \in V} C_{F_{v,t}} \right)$ s.t.	(8)
	$C_{U_{A_{e,t}}} \geq \hat{u}_e(\phi_{e,t} - z_{e,t}),$	$\forall e, t$ (17)
	$C_{U_{K_{e,t}}} \geq \hat{u}_e(\theta_{e,t} - z_{e,t}),$	$\forall e, t$ (18)
	$\theta_{e,t} \geq \frac{1}{n_K n_\tau} \sum_{\tau=1}^{n_\tau} q_{e,\tau,t},$	$\forall e, t$ (22)
	$f_{v,t} \leq p_{v,t}, \quad q_{v,1,t} = f_{v,t}, \quad q_{v,n_\tau,t} = f_{v,t},$	$\forall v, t$ (24)
	$\sum_{l \in L} q_{l,\tau,t} = \sum_{v \in V} f_{v,t},$	$\forall \tau, t$ (25)
	$l_{ij} = \sum_{(v_i, v_j) \in L} q_{l_{ij}, \tau-1, t} = \sum_{l_{ji} = (v_j, v_i) \in L} q_{l_{ji}, \tau, t},$	$\forall t, v_j, \tau \in [2, n_\tau]$ (27)
	$\delta_{e,t} \leq \sum_{\tau=1}^{n_\tau} q_{e,\tau,t},$	$\forall e, t \in [1, n_T - 2]$ (28)
	$z_{e,t} \leq \sum_{t_h=\max(t-\lambda,1)}^{t-1} \delta_{e,t_h} \frac{\lambda - (t - t_h) + 1}{\lambda(t - t_h)},$	$\forall e, t$ (30)
	$\psi_t \geq \frac{1}{n_A + n_K n_\tau} \sum_{e \in E} \left( p_{e,t} + \sum_{\tau=1}^{n_\tau} q_{e,\tau,t} \right),$	$\forall t$ (21)
	$\phi_{e,t} \geq \frac{1}{n_A} p_{e,t},$	$\forall e, t$ (22)
	$p_{s,1} = n_s, \quad p_{d,n_T} \geq n_d$	$\forall s, d$ (23)
	$\sum_{l \in L} p_{l,t} = n_A,$	$\forall t$ (25)
	$l_{ij} = \sum_{(v_i, v_j) \in L} p_{l_{ij}, t-1} = \sum_{l_{ji} = (v_j, v_i) \in L} p_{l_{ji}, t},$	$\forall v_j, t \in [2, n_\tau]$ (26)

cost reduction. In the following examples, we use demonstrative values for the parameters in Table I. For a particular scenario, parameters  $\xi$ ,  $\lambda$ , and  $\beta$ , as well as any weights added to the cost functions, are set based on the desired risk tolerance, completeness of exploration, and/or frequency of exploration. In particular,  $\xi$  controls the prioritization of exploring all edges versus edges planned to be traversed, smaller  $\lambda$  values will trigger more frequently revisiting explored edges, and  $\beta$  reflects the tolerance of risk (closer to 0 being the most risk averse). Unless noted otherwise, in the following examples we used  $\xi = 1$ ,  $\lambda = 5$ , and  $\beta = 0$ . With the exception of the ablation study, we construct graphs with randomly generated expected edge costs and uncertainty to evaluate our algorithm; however, we note that these values could be generated from continuous space as in [34].

#### A. Ablation Study

To demonstrate the advantages of each component of our algorithm, we performed an ablation study on the example graph in Fig. 2. We consider symmetric uncertainty about an expected value of each edge weight. The true values can be observed by the scouts and evolve (e.g., due to the observer moving), so frequent exploration will yield updated values. All robot units (carrier robots with scouts) start at node 0. The overall goal is for some subset of units to reach node 7 within 8 time steps  $t$ . The cost reduction for teaming,  $r_e$ , is 1 on all edges to incentivize moving together (though reducing uncertainty is often more valuable). Scouts can move 8 scout time steps,  $\tau$ , within one time step,  $t$ . Scouts' movement costs a quarter of the cost of an edge (weight and uncertainty) (i.e.,  $\zeta = 0.25$ ), as they would be less detectable. Fig. 3 depicts the final team paths and true cost for the route to the goal



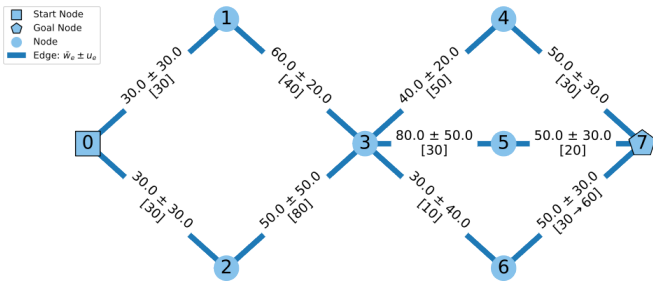


Fig. 2. Example dynamic topological graph with expected edge weights, uncertainty, and the true cost (in brackets) labeled for each edge. The true cost of edge (6,7) changes over time from 30 to 60.

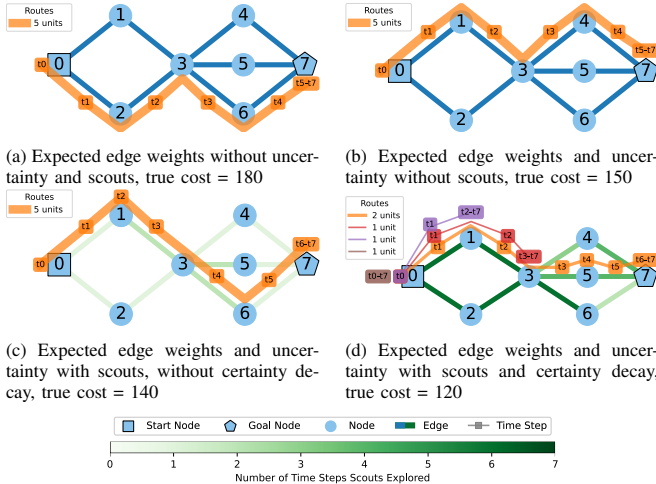


Fig. 3. Ablation study illustrating the advantages of considering uncertainty, scouts for the reduction of uncertainty, and certainty decay for evolving conditions. Each plot shows the final paths of the robot units through the graph. Each unit is composed of a robot carrier and scout. The first case is the baseline from [2] and each subsequent case adds one of the components from the algorithm proposed in this paper to show the resulting effect to the final team routes through the graph. In (c) and (d), the darkness of the edges reflect the number of time steps the scouts explored that edge.

node for each ablation case where the noted elements were removed from our optimization problem in Table III.

In Fig. 3a, the path with minimum expected edge cost is selected. However, the high uncertainty results in a high true cost. When the uncertainty is considered in Fig. 3b, a path that minimizes the expected weights and the maximum uncertainty is found. This plans for a worst-case scenario. In Fig. 3c, scouts are deployed at nodes 0 and 1 to reduce the uncertainty in planning. The scout paths are shown in Fig. 4. These deployments result in a more informed route, however, conditions are continuously evolving, and exploring each location once is not sufficient to see the future cost increase associated with traversing edge (6,7). Finally, we introduce decaying certainty to our algorithm in Fig. 3d, such that uncertainty increases after a scout visit to incentivize revisiting locations for updated information. This results in a team plan that minimizes the true cost. In this case, the benefit of frequent scout deployments outweighed traversing together, which resulted in units staying behind at nodes. This ablation study emphasizes the differences between each ablation case; however, the cost function can be weighted differently based on the priorities of a scenario.

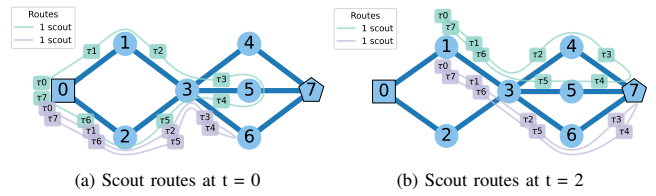


Fig. 4. Scout routes when deployed in the ablation case in Fig. 3c.

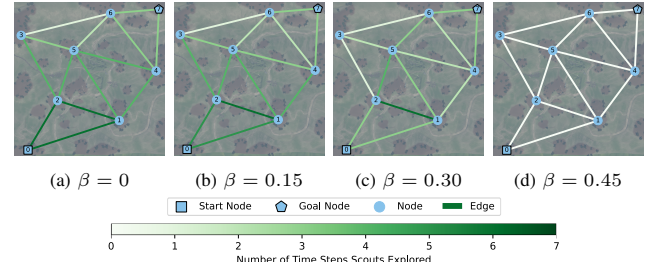


Fig. 5. Scout exploration for different coefficients of optimism,  $\beta$ .

### B. Coefficient of Optimism

Our coefficient of optimism  $\beta$  from the Hurwicz Criterion reflects our tolerance of risk. Setting  $\beta = 0$  is the most risk averse approach and considers the uncertainty in the worst-case scenario. This results in scouts exploring more to reduce the overall risk. Fig. 5 shows the frequency scouts explore each edge for various  $\beta$  values.  $\beta$  could be set based on the operational scenario and tolerance for risk.

### C. Combinatorial Considerations and Computation Time

We investigated how the computation time of our algorithm scales with the number of decision variables when we apply our key innovations (removing the decision space dependence on the number of agents and the linear formulation of our cost functions and constraints). Our total number of decision variables scales by  $n_T(1+n_L+n_E+n_Ln_\tau+5n_E+n_V)$ . The greatest impact is due to the scout time step,  $\tau$ , occurring within each carrier robot time step,  $t$ .

To adjust for new information and an evolving environment, we plan in a receding horizon. At each time step, we generate optimal solutions for the remainder of our time horizon after updating our graph with the information gathered by the scouts. For real-time operation, we plan for the next step while the current step is executing. For these types of long distance plans ( $\sim 100 - 250m$  edges), traversing one edge can take numerous minutes, so our computational requirement is to solve for a new plan in less time. To demonstrate the scaling of our approach, we plot the computation time for each iteration on three differently sized graphs versus the number of decision variables in Fig. 6. Graph 1 is shown in Fig. 1 and Graph 3 is shown in Fig. 5. When planning through an environment, the data points in Fig. 6 occur right to left, with the total number of decision variables decreasing with the receding horizon. We averaged computation times across 100 trials with randomized edge weights and uncertainty. We used the Gurobi optimizer [39] on an Intel® Core™ i7-10875H CPU @ 2.30GHz  $\times$  16. The longest computation time remains on the order of seconds, which enables regular re-planning.

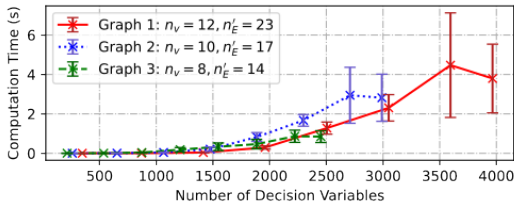


Fig. 6. Computation time for three example graphs of varying sizes versus the number of decision variables. Error bars are one standard deviation.

## VI. CONCLUSION

In this paper, we explored multi-robot planning on dynamic topological graphs using mixed-integer programming for two challenging cases: heterogeneous teams and planning under uncertainty. We use the uncertainty in our problem as a motivation for a heterogeneous team, introducing scout robots that can investigate the environment to collect data and reduce the uncertainty of future team actions. Our approach results in a MILP problem that can be solved rapidly with a receding horizon in real-world scenarios. We tested this approach in example scenarios and demonstrate the ability to successfully generate risk-aware plans for multi-robot teams.

## ACKNOWLEDGMENT

We gratefully acknowledge the support of the Army Research Laboratory under grant W911NF-22-2-0241.

## REFERENCES

- [1] Nature Manufacture, “Meadow - Environment Set.” [Online]. Available: <https://naturemanufacture.com/meadow-environment-set/>
- [2] C. A. Dimmig, K. C. Wolfe, and J. Moore, “Multi-Robot Planning on Dynamic Topological Graphs Using Mixed-Integer Programming,” in *Int. Conf. Int. Rob. Syst. (IROS)*, 2023, pp. 5394–5401.
- [3] K. Zhang, Z. Yang, and T. Basar, “Multi-Agent Reinforcement Learning: A Selective Overview of Theories and Algorithms,” *Handbook of Reinforcement Learning and Control*, vol. 18, p. 321, 2021.
- [4] C. H. Papadimitriou and J. N. Tsitsiklis, “The Complexity of Markov Decision Processes,” *Math. of Ops. Res.*, vol. 12, no. 3, pp. 441–450, 1987.
- [5] J. Capitan, M. T. Spaan, L. Merino, and A. Ollero, “Decentralized multi-robot cooperation with auctioned POMDPs,” *Int. J. Rob. Res.*, vol. 32, no. 6, pp. 650–671, 2013.
- [6] V. Indelman, “Cooperative multi-robot belief space planning for autonomous navigation in unknown environments,” *Aut. Rob.*, vol. 42, pp. 353–373, 2018.
- [7] M. J. Mataric, G. S. Sukhatme, and E. H. Østergaard, “Multi-robot task allocation in uncertain environments,” *Aut. Rob.*, vol. 14, pp. 255–263, 2003.
- [8] B. Woosley, C. Nieto-Granda, J. G. Rogers, N. Fung, and A. Schang, “Bid prediction for multi-robot exploration with disrupted communications,” in *Int. Symp. on Saf., Sec., and Resc. Rob.*, 2021, pp. 210–216.
- [9] M. Liu, K. Sivakumar, S. Omidshafiei, C. Amato, and J. P. How, “Learning for multi-robot cooperation in partially observable stochastic environments with macro-actions,” in *Int. Conf. Int. Rob. Syst. (IROS)*, 2017, pp. 1853–1860.
- [10] H. Ma, “Graph-based multi-robot path finding and planning,” *Curr. Rob. Rep.*, vol. 3, no. 3, pp. 77–84, 2022.
- [11] M. Limbu, Z. Hu, S. Oughourli, X. Wang, X. Xiao, and D. Shishika, “Team Coordination on Graphs with State-Dependent Edge Costs,” in *Int. Conf. Int. Rob. Syst. (IROS)*, 2023, pp. 679–684.
- [12] C. H. Papadimitriou and M. Yannakakis, “Shortest paths without a map,” *Theo. Comp. Sci.*, vol. 84, no. 1, pp. 127–150, 1991.
- [13] R. P. Loui, “Optimal Paths in Graphs with Stochastic or Multidimensional Weights,” *Comm. of the ACM*, vol. 26, no. 9, p. 670–676, Sept 1983.
- [14] G. H. Polychronopoulos and J. N. Tsitsiklis, “Stochastic shortest path problems with recourse,” *Networks*, vol. 27, no. 2, pp. 133–143, 1996.
- [15] D. P. Bertsekas and J. N. Tsitsiklis, “An Analysis of Stochastic Shortest Path Problems,” *Math. of Ops. Res.*, vol. 16, no. 3, pp. 580–595, 1991.

- [16] J. J. Chung, A. J. Smith, R. Skeele, and G. A. Hollinger, “Risk-aware graph search with dynamic edge cost discovery,” *Int. J. Rob. Res.*, vol. 38, no. 2-3, pp. 182–195, 2019.
- [17] S. Choudhury, J. K. Gupta, M. J. Kochenderfer, D. Sadigh, and J. Bohg, “Dynamic multi-robot task allocation under uncertainty and temporal constraints,” *Aut. Rob.*, vol. 46, no. 1, pp. 231–247, 2022.
- [18] O. Peltzer, K. Brown, M. Schwager, M. J. Kochenderfer, and M. Sehr, “STT-CBS: A conflict-based search algorithm for multi-agent path finding with stochastic travel times,” *arXiv preprint arXiv:2004.08025*, 2020.
- [19] S. Omidshafiei, A. Agha-Mohammadi, C. Amato, S. Liu, J. P. How, and J. Vian, “Decentralized control of multi-robot partially observable Markov decision processes using belief space macro-actions,” *Int. J. Rob. Res.*, vol. 36, no. 2, pp. 231–258, 2017.
- [20] M. Lauri, J. Pajarinen, and J. Peters, “Multi-agent active information gathering in discrete and continuous-state decentralized POMDPs by policy graph improvement,” *Auto. Agents and Multi-Agent Sys.*, vol. 34, no. 2, p. 42, 2020.
- [21] S. Bhattacharya, S. Kailas, S. Badyal, S. Gil, and D. Bertsekas, “Multiagent Reinforcement Learning: Rollout and Policy Iteration for POMDP with Application to Multi-Robot Problems,” *IEEE Trans. Rob.*, pp. 1–20, 2023.
- [22] M. Tzes, N. Bousias, E. Chatzipantazis, and G. J. Pappas, “Graph neural networks for multi-robot active information acquisition,” in *Int. Conf. Rob. Aut. (ICRA)*, 2023, pp. 3497–3503.
- [23] H. Zhang, J. Cheng, L. Zhang, Y. Li, and W. Zhang, “H2GNN: Hierarchical-hops graph neural networks for multi-robot exploration in unknown environments,” *IEEE Robot. Autom. Lett.*, vol. 7, no. 2, pp. 3435–3442, 2022.
- [24] P. Buchholz and I. Dohndorf, “Optimal decisions in stochastic graphs with uncorrelated and correlated edge weights,” *Computers & Operations Research*, vol. 150, p. 106085, 2023.
- [25] T. Okubo and M. Takahashi, “Multi-Agent Action Graph Based Task Allocation and Path Planning Considering Changes in Environment,” *IEEE Acc.*, vol. 11, pp. 21160–21175, 2023.
- [26] B. A. Asfora, J. Banfi, and M. Campbell, “Mixed-Integer Linear Programming Models for Multi-Robot Non-Adversarial Search,” *IEEE Robot. Autom. Lett.*, vol. 5, no. 4, pp. 6805–6812, Oct 2020.
- [27] M. Koes, I. Nourbakhsh, and K. Sycara, “Heterogeneous multirobot coordination with spatial and temporal constraints,” in *AAAI Conf. on Artificial Intelligence*, vol. 5, 2005, pp. 1292–1297.
- [28] N. Atay and B. Bayazit, “Mixed-Integer Linear Programming Solution to Multi-Robot Task Allocation Problem,” *Washington University, St. Louis Report Number WUCSE-2006-54*, 2006.
- [29] M. Lippi and A. Marino, “A Mixed-Integer Linear Programming Formulation for Human Multi-Robot Task Allocation,” in *Intl. Conf. on Rob. & Hum. Int. Comm. (RO-MAN)*, Aug 2021, pp. 1017–1023.
- [30] K. Leahy, Z. Serlin, C.-I. Vasile, A. Schoer, A. M. Jones, R. Tron, and C. Belta, “Scalable and Robust Algorithms for Task-Based Coordination From High-Level Specifications (ScRATHeS),” *IEEE Trans. Rob.*, vol. 38, no. 4, pp. 2516–2535, Aug 2022.
- [31] Z. Wang, C. Liu, and M. Gombolay, “Heterogeneous graph attention networks for scalable multi-robot scheduling with temporospatial constraints,” *Aut. Rob.*, pp. 1–20, 2022.
- [32] S. Paul, P. Ghassemi, and S. Chowdhury, “Learning Scalable Policies over Graphs for Multi-Robot Task Allocation using Capsule Attention Networks,” in *Int. Conf. Rob. Aut. (ICRA)*, May 2022, pp. 8815–8822.
- [33] H. Wu, A. Ghadami, A. E. Bayrak, J. M. Smereka, and B. I. Epureanu, “Impact of heterogeneity and risk aversion on task allocation in multi-agent teams,” *IEEE Robot. Autom. Lett.*, vol. 6, no. 4, pp. 7065–7072, 2021.
- [34] C. A. Dimmig, A. Goertz, A. Polevoy, M. Gonzales, B. Yeh, K. C. Wolfe, B. Woosley, J. G. Rogers III, and J. L. Moore, “Multi-Robot Planning for Coordinated Off-road Maneuvers,” in *ICRA Workshop on Resilient Off-road Autonomy*, 2024.
- [35] T. Denœux, “Decision-making with belief functions: A review,” *Int. J. of Approx. Reas.*, vol. 109, pp. 87–110, 2019.
- [36] M. Hurwicz, “The Hurwicz Criterion.” [Online]. Available: <https://www.leonidhurwicz.org/hurwicz-criterion/>
- [37] F. Glover, “Improved linear integer programming formulations of nonlinear integer problems,” *Management Science*, vol. 22, no. 4, pp. 455–460, 1975.
- [38] W. P. Adams and R. J. Forrester, “A simple recipe for concise mixed 0-1 linearizations,” *Ops. Res. Lett.*, vol. 33, no. 1, pp. 55–61, 2005.
- [39] Gurobi Optimization, LLC, “Gurobi Optimizer Reference Manual,” 2023. [Online]. Available: <https://www.gurobi.com>